Since January 2020 Elsevier has created a COVID-19 resource centre with free information in English and Mandarin on the novel coronavirus COVID-19. The COVID-19 resource centre is hosted on Elsevier Connect, the company's public news and information website.

Water Research 196 (2021) 117033

Contents lists available at ScienceDirect

Water Research

journal homepage: www.elsevier.com/locate/watres

An investigation into the leaching of micro and nano particles and chemical pollutants from disposable face masks - linked to the COVID-19 pandemic

G.L. Sullivan [a], J. Delgado-Gallardo [b], T.M. Watson [a], S. Sarp [b,*]

[a] SPECIFIC, College of Engineering, Swansea University, SA2 8PP, UK
[b] SPEC, College of Engineering, Swansea University, SA2 8PP, UK

ARTICLE INFO

Article history:
Received 9 February 2021
Revised 5 March 2021
Accepted 8 March 2021
Available online 10 March 2021

ABSTRACT

The production of disposable plastic face masks (DPFs) in China alone has reached to approximately 200 million a day, in a global effort to tackle the spread of the new SARS-CoV-2 virus. However, improper and unregulated disposals of these DPFs has been and will continue to intensify the plastic pollution problem we are already facing. This study focuses on the emission of pollutants from 7 DPF brands that were submerged in water to simulate environmental conditions if these DPFs were littered. The DPF leachates were filtered by inorganic membranes, and both particle-deposited organic membranes and the filtrates were characterized using techniques such as FTIR, SEM-EDX, Light Microscopy, ICP-MS and LC-MS. Micro and nano scale polymeric fibres, particles, siliceous fragments and leachable inorganic and organic chemicals were observed from all of the tested DPFs. Traces of concerning heavy metals (i.e. lead up to 6.79 μg/L) were detected in association with silicon containing fragments. ICP-MS also confirmed the presence of other leachable metals like cadmium (up to 1.92 μg/L), antimony (up to 393 μg/L) and copper (up to 4.17 μg/L). LC-MS analysis identified polar leachable organic species related to plastic additives and contaminants; polyamide-66 monomer and oligomers (nylon-66 synthesis), surfactant molecules, dye-like molecules and polyethylene glycol were all tentatively identified in the leachate. The toxicity of some of the chemicals found and the postulated risks of the rest of the present particles and molecules, raises the question of whether DPFs are safe to be used on a daily basis and what consequences are to be expected after their disposal into the environment.

1. Introduction

The SARS CoV-2 pandemic has caused an unprecedented rise of face mask wearing in order to mitigate the spread of this airborne viral disease (Wilson et al., 2020), as recommended by the World Health organisation (WHO)(Adyel, 2020; Aragaw, 2020; Fadare and Okoffo, 2020). This has seen an increase in mass production of face coverings to keep up with global demand. The WHO has estimated an additional 89 million disposable plastic face masks (DPFs) are required a month in order to protect health care workers alone (Aragaw, 2020; Fadare and Okoffo, 2020). Presently, China is the main manufacturer and distributer of DPFs, with an estimated production of 200 million DPFs per day (Aragaw, 2020), with up to a 1 billion DPFs being used globally on a monthly basis (Adyel, 2020). This has seen a notable increase in DPF and clinical waste, irresponsibly discarded and disposed at landfill sites; with a large proportion inevitably ending up in the water course and the ocean (Fadare and Okoffo, 2020). The rise in DPFs waste is regarded as a new cause of pollution directly linked COVID-19 pandemic. However, there is still very little data on the effect of the pollution caused by DPFs on the wider environment (Adyel, 2020).

Most DPFs are made entirely from plastic fibres (Aragaw, 2020; Jung et al., 2021), containing high percentages of polypropylene (PP) and polyethylene (PE), and other polymeric materials such as nylon and polystyrene (Aragaw, 2020; Fadare and Okoffo, 2020; Jung et al., 2021) with novelty face masks often coloured with dyes for customer appeal. The manufacturing of DPFs often involves electrospinning micro and nanofibres of plastic, into three layers (Aragaw, 2020; Fadare and Okoffo, 2020). In some manufacturing processes, silica nano particles maybe added as filler to enhance plastic properties such increasing mechanical strength and toughness of the material (Wu et al., 2005).

There is a growing concern around the environmental fate of DPFs and whether they emit pollutants such as microscopic

* Corresponding author.
E-mail address: sarper.sarp@swansea.ac.uk (S. Sarp).

https://doi.org/10.1016/j.watres.2021.117033
0043-1354/

polymeric fibres (Aragaw, 2020; Fadare and Okoffo, 2020), microcrystalline silica and other secondary pollutants, such as leachable chemicals (dyes, surfactants and glues). There is little information on the environment impacts of these pollutants and whether they may enter the food chain. Many of these chemical dyes are associated with heavy inorganic metals (Sungur and Gülmez, 2015) and are known to have an adverse impact on the environmental and potentially human health. Metals such as antinomy (Sb), copper (Cu) and chromium (Cr) are used as catalysts in dye manufacture and sometime residues are found in textiles materials as plastic additives (Hahladakis et al., 2018; Sungur and Gülmez, 2015). Some reactive dyes also form complexes with heavy metals, such as nickel (Ni), Cu and Cr. These chemicals may be associated with particles that can be transmitted from the face masks and enter the respiratory track via inhalation or absorbed through skin contact; these chemicals may dissolve in moisture droplets of sweat and saliva, which may act as a medium for transport into the body. There are known hazards associated with these chemicals, especially heavy metals, ranging from mild allergic reactions, often from limited exposure, to more serious health issues from repeated exposure; such as renal disease, emphysema, cancer and often may be harmful to unborn children in pregnancy (Sungur and Gülmez, 2015; Tchounwou et al., 2012).

Dye compounds themselves pose risk to environmental and public health (Lellis et al., 2019). As many of them are water soluble organic molecules and leachable, they can therefore enter the water course and food chain. Most dyes are also chromophores, competing for light in the environment and reducing the photosynthesis of aquatic plants, and thus disrupting the ecosystem (Lellis et al., 2019). Due to the polarity of these molecules, they are often difficult to remove by conventional water treatment methods, ending up in drinking water (Lellis et al., 2019). Most of these compounds have carcinogenic and mutagenic properties as they are, generally, highly aromatic. Furthermore, these dye molecules have the ability to enter cells and intercalate with the cell's DNA, disrupting transcription processes of the cell (Lellis et al., 2019). Most dye compounds are deemed as persistent organic pollutants and have the potential to bioaccumulate in many species, including humans (Lellis et al., 2019).

Not only chemical species but also the release of submicron particles from DPFs are cause of concerns. Recent studies of micro plastic (MPs)(>5 mm), and nano plastics (NP) (>1 μm), (Bianco and Passananti, 2020; Paul et al., 2020; Toussaint et al., 2019) which included polymeric fibres, showed that they have detrimental effects in animal models. MPs and NPs exhibit cytotoxic and genotoxic effects in terrestrial (including humans) and aquatic organisms (Bouwmeester et al., 2015). In recent articles, researchers have shown that some MPs and NPs can be adsorbed by the gut and then passed through the blood brain barrier (Kögel et al., 2020; Lusher et al., 2017) resulting in neurotoxic damage (Prüst et al., 2020). These particles often produce cellular damage by causing increased oxidative stress, as the particles are recognised by the organism as being foreign (Bhagat et al., 2020; Prüst et al., 2020). In one report, fibres were found to embed themselves easier in tissues rather than spherical particles. The result of which caused increased superoxide dismutase levels in gut tissue of zebra fish, an indication of oxidative stress and inflammation (Bhagat et al., 2020). Further to this, there is also evidence to suggest that NPs may be small enough to penetrate the cell wall, releasing persistent organic pollutants into tissues (Bhagat et al., 2020; Bouwmeester et al., 2015), or they can be activated NP particles, containing reactive sites on chain ends, which can inflict DNA damage. These effects can cause cell death, genotoxicity, or cancer formation.

Additional to this, there is a potential human health concern around the presence of micro silica particles (SiMP) between 1 and 10 μm and nano silica particles (SiNP) <1 μm, which is often used in manufacturing process of plastics (Masuki et al., 2020; Murugadoss et al., 2017). There is strong evidence to support the human health implications of crystalline and amorphous silica if inhaled; this silica nano particles can cause lung irritation and silicosis (fibrosis of the lung) which can develop into emphysema and lung cancer (Lin et al., 2006; Masuki et al., 2020; Murugadoss et al., 2017). SiMP and SiNP cause cell damage through oxidative stress, that leads to DNA damage, genotoxicity and cell death (Murugadoss et al., 2017). SiMP and SiNP toxicity is also evident in other tissues, causing cancers in blood and bone tissue and causing neurotoxicity in brain tissues (Masuki et al., 2020; Murugadoss et al., 2017; You et al., 2018). However, SiMP and SiNP have lower environmental impact with mild toxic effects seen in aquatic organisms and terrestrial animals if ingested (Fruijtier-Pölloth, 2012). Nevertheless, the presence of these particles in DPFs water leachates, may be indicative of the ease of their discharge. This could raise further concerns regarding their potential release when wearing face coverings; could they be easily inhaled?

The aim of this investigation is to identify the environmental impact of DPFs when disposed improperly, via formalizing a workflow procedure to characterize various pollutants emitted/leached from DPFs (Song et al., 2015; Sullivan et al., 2020) during simulated environmental conditions (face mask gently agitated in deionised water).

Fig. 1. Shows images of the typical face masks used in this investigation. Image 1 corresponds to face mask 1; standard plain face mask (similar to face mask 3, 5 and 6), image 2; face mask 2 (black color), Image 4; face mask 4 (novelty kids), Image 7a- c; face masks 7a-c (Festive face masks).

2. Materials and methods

2.1. Materials and instrumentation

The following lists the consumables and instrumentation used in the present investigation:

DPFs were purchased from several manufacturers and suppliers as listed in Table 1 and Fig. 1, and contaminants were extracted using deionised water dispensed from Milli Q® type 1 dispenser, procedural blanks were also prepared using the same deionised water source. Whatman® Anodisc inorganic membranes of 0.1 μm pore size (Merck Group® UK) were used as membrane filters for particle deposition. A Glass vacuum manifold purchased from Sigma Aldrich®UK and vacuum pump Sparmax (The Airbrush Company Ltd, UK) were used to aid filtration of leachate. For microscopy analysis, a Zeiss Primotech light microscope (Carl Zeiss Ltd., Cambridge, UK) and TM3000 SEM electron microscope (Hitachi High-Technologies Corporation) were used for particle identification.

A Perkin Elmer® FTIR Frontier (UK) was used for chemical characterization of solid materials and a Perkin Elmer® ICP-MS NexIon 2000 for metal leachate identification and quantification. An Agilent® (UK) 1100 and Dionex ultimate® (UK) 3000 was used

Table 1
Shows the information associated with various DPFs analysed and supplier purchased from.

Sample	Description	Brand	Manufacturer	Distributor	Type	Supplier
Face Mask 1	Plain	NA	Huaxian Tiancheng Sanitary Material Co., Ltd	NA	NA	Amazon
Face Mask 2	Black	PRO SFE	Shanghai Careus Medical Product Co., Ltd	Hunter Price International	NA	Poundland
Face Mask 3	Plain children	PMS International	NA	NA	NA	CKs store
Face Mask 4	Novelty children (paw patrol)	NA	Guangzhou Quantum Laser Intelligent Equipment co., Ltd	Sambro International Ltd.	Type I	Poundland
Face Mask 5	Plain	TLS	Toiletry Sales Ltd	Toiletry Sales Ltd	Type IIR	Sainsbury
Face Mask 6	Plain	CGM-3PLY	Foshan Suncare Medical Products Co., Ltd	Teucer (UK) Ltd	NA	Tesco
Face Mask 7a Face Mask 7b Face Mask 7c	Festive Red Festive blue Festive green	NA	Shanghai Ogo Medical Instrument Co., Ltd	Sambro International Ltd.	Type I	Poundland

for LCMS analysis of organic contaminates, which were tentatively identified using a Thermo LTQ Orbitrap XL accurate Mass spectrometer. For chromatographic separation a reverse phase XBridge C18 column with dimensions: 3.5 µm x 2.1 mm x 150 mm and Guard column: XBridge C18 3.5 µm x 2.1 mm x 10 mm was used.

2.2. Methodology

2.2.1. Leaching and filtration of particles

For particle analysis, 10 face masks for each batch were submerged in 1.5 L deionised water for 4 h and gently agitated by stirring every hour to ensure complete coverage and contact of DPFs with water. Post submersion, the eluent (leachate) was then filtered under vacuum through a 0.1 µm Al_2O_3 membrane filter. Once complete, the membranes were then transferred to glass petri dishes for drying in a drying cabinet for 2 h at 50 ° C. Procedural blanks were also run with each batch, this involved filtering 1.5 L of deionised water only, through the membranes and then drying for 2 h at 50 ° C. The filtration process was carried out using a glass vacuum filtration funnel and receiving flask with samples drawn through under negative pressure (Sullivan et al., 2020).

2.2.2. Microscopy

Light microscopy of the membranes was used to determine coverage of particle contamination, this was done using Zeiss Primotech microscope (Carl Zeiss Ltd., Cambridge, UK) at 5 x, 10 x and 50 x magnification.

For scanning electronic microscopy (SEM) and energy-dispersive X-ray spectroscopy (EDX) analysis, a Tabletop Microscope TM3000 was utilized (Hitachi High-Technologies Corporation), samples were mounted on carbon tape and placed in vacuums chamber prior.

2.2.3. FTIR characterization of DPFs and membrane

Surface characterization was carried out using a Perkin Elmer FTIR Frontier for rapid solid sample analysis. Solid material placed over crystal housing and pressed down using the gage with a force of 30 (arbitrary units). Scan was between 650 and 4000 cm^3, with 4 accumulations per second, to get an average spectrum.

2.2.4. ICP-MS elemental analysis

Selected DPFs were placed in 250 mL deionised water and left submerged for 24 h typical of leachate analysis in environmental laboratories. The leachate was then subsampled and acidified using 1 mL of 1 M nitric acid and run on Perkin Elmer ICP-MS NexIon 2000 a standard procedure for elemental analysis. A procedural blank (deionised water passed through membrane) and reagent blank (deionised water only) was run with samples to check for background interference. Blanks were run after highest calibration and after every sample to check for carryover.

Multielement calibration standards, representing all the analytes in the sample, were made up from PerkinElmer Pure single and multielement standards and diluted into 10% HNO3. Calibration range of 1 µg/L to 100 µg/L was preformed and standard curve required regression statistics above 0.9990 to be deemed acceptable, samples exceeding 100 µg/L were diluted accordingly to bring into dynamic range. Quality control samples prepared from separate batch of multielement standards and prepared at 50% of calibration range, acceptance criteria for accuracy and precision was deemed acceptable below 15%. Instrument parameters as follows: plasma gas flow set at 18 L/minute of argon, auxiliary gas flow set at 1.8 L /minute and nebuliser flow rate of set at 0.98 L/minute. Sample uptake was set at 300 µL/minute with 3 replicates per sample, the RF voltage was applied at 1600 W, as determined by method optimization during method development (Hineman and Purcell-joiner, 2010).

2.2.5. LC-UV and LC-MS accurate mass of leachate

A subsample of the leachate described in 2.1.4 was analysed for polar organic compounds by direct injection (5 µL) on LC-UV for initial sample contamination screening and LC-MS for compound identification. LC-UV was run using Agilent 1100 and a dionex ultimate 3000 for LCMS. A Waters XBridge C18 column: 3.5 µm x 2.1 mm x 150 mm and Guard column: XBridge C18 3.5 µm x 2.1 mm x 10 mm was used for analyte separation for both systems and used a Flow rate 200 µl/min for LC/UV; 150 µl/min for LC/MS. The composition of mobile phase A was 0.1% Formic acid; 2% (Acetonitrile) MeCN in (Water) H_2O and mobile phase B 0.1% Formic acid in MeCN for both instrument set-ups. The elution gradient started at 2% B and increased to 90% at 32 min before returning to 2% B ending with a total run time of 37 min. For UV–VIS parameters the lamp was set at 254, 214 and 360 nm with bandwidth of 4, 16 and 32 nm respectively, compared to a reference cell set at 360 nm with bandwidth of 100 nm. The DAD spectrum operated at bandwidth of 190–700 with a refenced at bandwidth of 2 nm.

For analysis: reagent blanks (LC grade water) and procedural blanks (deionised water used in sample preparation) were run before and after sample runs to check the background ions and potential carryover. A coumarin standard was also run as pre and post sample analysis to verify the system suitability i.e. retention time drift, analyte response and peak profile for coumarin.

For MS parameters, the dionex ultimate 3000 was connected in series to a Thermo LTQ Orbitrap XL with API ion spray source; sheath gas flow was set to 15 L/minute, auxiliary gas flow set at 2 L per minute, the probe was voltage was set at 4.3 kV with capillary and tube lens voltage of 43 and 150 V respectively. MS scan conditions was full mass profile mode *m/z* 200–1000 with resolution of 60,000. LCMS was tuned and calibrated using infusion at low flow rate of tune mix, containing a mixture of caffeine, MRFA and ultra Mark (Cal mix) prior to each analysis. A coumarin standard was also used to optimize parameters of LC flow rate. Reagent and procedural blanks were also run prior and post sample analysis to establish background of the system.

3. Results and discussion

3.1. Face mask and filtrate characterization: microscopy and FTIR analysis

9 separate batches of DPFs (from 7 brands) (Fig. 1) were tested for their leaching potential of dispersive pollutants in water. The membranes from the filtration process were then subjected to Microscopy (SEM-EDX and light microscopy) and FTIR, for characterization. Light microscopy was used for an initial indication of particle contamination (Fig. 2); all 9 batches of DPFs (Face mask 1 to 7c) emitted fibres believed to be PP and angular fragments that seemed to have crystalline appearance, suspected to be of siliceous composition. It appears that Novelty children face mask 4 and Novelty festive face masks 7a-c have significant fiber and particle contaminations. Light microscopy images of 7 a-c show many different coloured fibres, suggesting that some are stained with a dying agent and looks as though the membrane filters are also slightly tarnished. This is true for face mask 2, although in less abundance than 4, 7 a-c, the fibres are predominantly black (in line with ap-

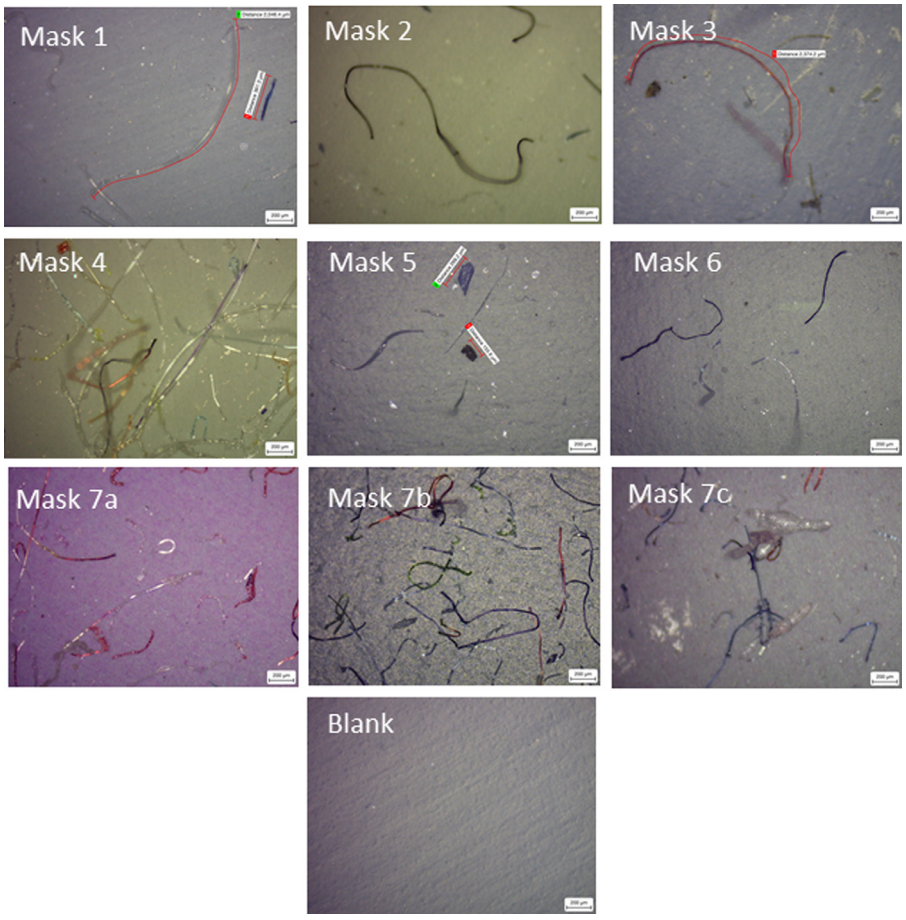

Fig. 2. Light microscope images of the membrane filters post filtration of face masks1–7c taken and blank membrane at 5 x magnification. Notably face mask 4 (paw patrol) and 7a-c (festive novelty) have what appears significant fibres and particle contamination.

Table 2
A table comparing the main FTIR absorbance peaks of the original physical DPF, with the filtered membrane supports. Peaks in red and blue font are peaks derived elsewhere other than PP.

Sample	Descriptor	FTIR main peaks of original face mask cm^{-1}	FTIR main peaks on membrane filter cm^{-1}
Blank	Membrane only	Not detected	Not detected
Face mask 1	Plain (Amazon)	2950 cm^{-1} 2917 cm^{-1} 2838 cm^{-1} 1457 cm^{-1} 1375 cm^{-1}	Not detected
Face mask 2	Black colour	2950 cm^{-1} 2917 cm^{-1} 2838 cm^{-1} 1457 cm^{-1} 1375 cm^{-1}	2950 cm^{-1} 2917 cm^{-1} 2838 cm^{-1} 1711 cm^{-1} 1457 cm^{-1} 1015 cm^{-1} 1375 cm^{-1}
Face mask 3	Plain children	2950 cm^{-1} 2917 cm^{-1} 2838 cm^{-1} 1457 cm^{-1} 1375 cm^{-1}	3275 cm^{-1} 2950 cm^{-1} 2917 cm^{-1} 1025cm^{-1}
Face mask 4	Novelty children (paw patrol)	2950 cm^{-1} 2917 cm^{-1} 2838 cm^{-1} 1457 cm^{-1} 1375 cm^{-1} 1711 cm^{-1} 1242 cm^{-1} 1095 cm^{-1}	1711 cm^{-1} 1242 cm^{-1} 1095 cm^{-1}
Face mask 5	Plain (Sainsbury)	2950 cm^{-1} 2917 cm^{-1} 2838 cm^{-1} 1457 cm^{-1} 1375 cm^{-1}	None detected
Face mask 6	Plain (Tesco)	2950 cm^{-1} 2917 cm^{-1} 2838 cm^{-1} 1457 cm^{-1} 1375 cm^{-1}	None detected
Face mask 7 a	Festive Red	2950 cm^{-1} 2917 cm^{-1} 2838 cm^{-1} 1457 cm^{-1} 1375 cm^{-1} 1711 cm^{-1} 1242 cm^{-1} 1095 cm^{-1}	2950 cm^{-1} 2917 cm^{-1} 2838 cm^{-1} 1408 cm^{-1} 1339 cm^{-1} 1713 cm^{-1} 1240 cm^{-1} 1093 cm^{-1}
Face mask 7 b	Festive blue	2950 cm^{-1} 2917 cm^{-1} 2838 cm^{-1} 1457 cm^{-1} 1375 cm^{-1} 1711 cm^{-1} 1242 cm^{-1} 1095 cm^{-1}	2950 cm^{-1} 2917 cm^{-1} 1457 cm^{-1} 1375 cm^{-1} 1711 cm^{-1} 1242 cm^{-1} 1095 cm^{-1}
Face mask 7 c	Festive Green	2950 cm^{-1} 2917 cm^{-1} 2838 cm^{-1} 1457 cm^{-1} 1375 cm^{-1} 1711 cm^{-1} 1242 cm^{-1} 1095 cm^{-1}	1711 cm^{-1} 1242 cm^{-1} 1095 cm^{-1}

pearance of original face mask). Face masks 1, 3, 5 and 6 appear to generate lower number of fibres, in comparison with 4, 7a-c, and generate a mixture of clear and blue fibres (similar appearance of the original face masks).

FTIR analysis of the physical face masks confirms the manufacture of these masks are primarily out of PP, with some additional functionalisation seen of in the novelty face masks (4, 7 a b c), particularly on coloured sides. The white side presented spectrum indicative of PP; absorbance peaks 2950 cm^{-1} 2917 $cm^{-1}$are asymmetrical stretching of CH_3 and CH_2 respectively 2838 cm^{-1}, stretching CH_3, 1457 cm^{-1} and 1375 cm^{-1} are symmetrical stretching of CH_3. The coloured side showed primarily an absorption band at 1712 cm^{-1}, indicative of carboxylic acid or ketone functional (see Table 2). This could possibly arise from the side group of an acidic dye compound, polyamide used in synthesis of nylon −66 and sometimes found in oxidised PP (Charles et al., 2009; Coates, 2006; Jung et al., 2018). For plain face masks both blue and white side possessed peaks indicative of PP.

For the membrane supports post filtration, FTIR was performed on all 9 batches; absorbance spectrum in line with main peaks of PP were identified on membrane supports from face mask 2, 3 and 7 a b c, further supporting that membrane fibres derived from masks are PP in composition. For some face masks, less fibrous material was likely transferred to the support (i.e. face masks 1, 5 and 6 were plain typical medical type face masks as the detection of PP peaks where below the capabilities of the ATR-FTIR).

Additional peaks were identified in novelty face masks coloured side (4, 7 a b c): peaks 1711 cm^{-1}(carboxylic acid stretching), 1242 cm^{-1} (oxirane or sulfonic acid group) and 1095 cm^{-1}(secondary alcohol stretch) (Bartošová et al., 2017; Coates, 2006). They were also often seen as the primary peaks on the membranes post filtration, and are often common groups in dyes such as eriochrome black and congo red (Bartošová et al., 2017). These membranes were often tarnished, suggesting that these peaks are more than likely derived from the inks or dyes used in the printing of the novelty graphics.

More in-depth analysis of the membrane filters was preformed using SEM-EDX. It was confirmed that particle sized trapped on the support can be classified in micro particle (<1 mm) and nano (submicron particle size 0.1–1 μm) range with all face masks emitting significant amount of grain sized particles measured between 360 nm- 500 μm on SEM (Fig. 3), but likely to be even finer (limited by resolution of TM3000). Fibrous particles appeared to be in greater size range, often ranging from as little as 25 μm to several millimetres (2.5 mm). Fibres were found to be emitted from all face masks in this study (Masks 1–7c). Further to this EDX analysis using back scattered electrons suggested the elemental composition of particles. It was noted that fibrous particles had high percentage of carbon, most likely derived from polypropylene spun fibres. The majority of the grains contained high percentages of Si and oxygen and likely to be compositions of silica (Fig. 4). However, some grains analysed (thought to be silica) were often high in carbon and likely even finer fragments of plastics (Fig. 4).

Additional to this, there was often presence of heavy metals associated with these particles, especially in the novelty face masks

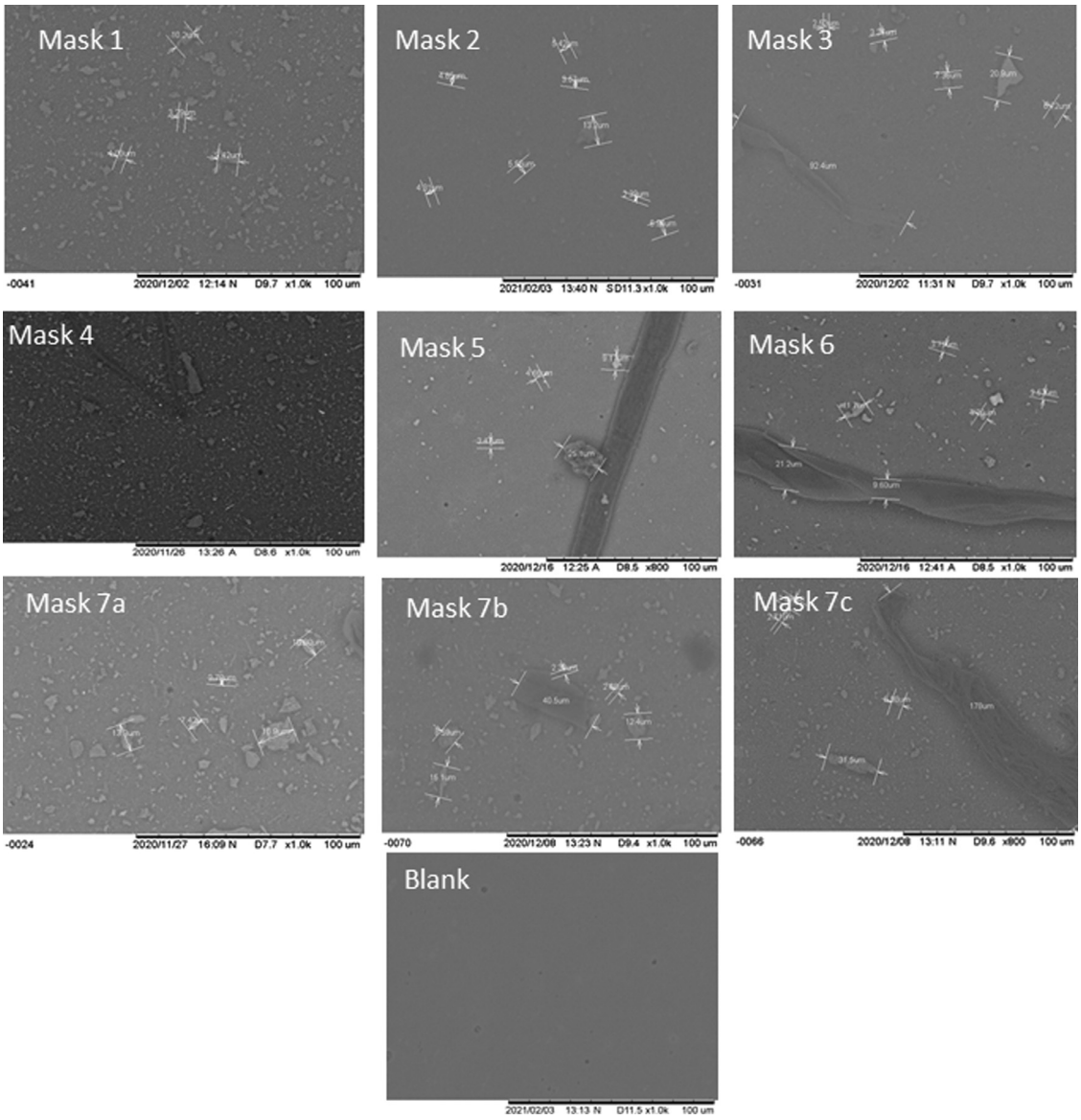

Fig. 3. SEM images of fibres and particles from face masks 1–7C and blank membrane filter. Elemental compositions of fibres were found to be mainly carbon, whilst the small angular fragments found in all face masks had high percentages of Silica and Oxygen. .

Table 3
Lists some of the main heavy metals discovered in the DPF leachate (250 mL). Face masks 7a, b, c appears to have the highest release of Sb, whilst Cu is released from all masks.

Sample	Cd (µg/L)	Co (µg/L)	Cu (µg/L)	Pb (µg/L)	Sb (µg/L)	Ti (µg/L)
Procedural Blank	N.D*	N.D	N.D	N.D	N.D	N.D
Face mask 2 (Leachate)	N.D	N.D	**4.17**	**0.01**	**1.06**	**0.64**
Face mask 4 (Leachate)	**0.01**	**0.54**	**1.87**	**0.62**	N.D	**0.27**
Face mask 4 (Leachate) repeat	**0.04**	**0.59**	**1.22**	**0.89**	N.D	N.D
Face mask 5 (Leachate)	N.D	N.D	**0.85**	**0.75**	**3.07**	N.D
Face mask 6 (Leachate)	**1.92**	N.D	**1.80**	**6.79**	N.D	N.D
Face mask 7 a (Leachate)	**0.53**	N.D	**2.06**	**1.62**	**111**	N.D
Face mask 7 b (Leachate)	N.D	N.D	**2.31**	N.D	**393**	**0.12**
Face mask 7 c (Leachate)	N.D	N.D	**4.00**	N.D	**147**	**0.06**

* *Not Detected.*

such as masks 2, 4, 7a, b, c. Some heavy metals were located on grain particles as seen in masks child's novelty face mask (4) shown in Fig. 5 and the festive face masks (7 a, b, c), and likely additives used in plastic manufacture. Heavy metals associated fibres are common chemical additives added during plastic manufacture such as Pb, Cd, Sb and Cu (Hahladakis et al., 2018).

3.2. Leachable metals and organic compounds: ICP-MS and LC-MS analysis

It was apparent from EDX analysis that heavy metals were associated mainly with coloured novelty face masks. It was therefore decided to analyze the coloured masks (face masks 2, 4, 7a, b, c)

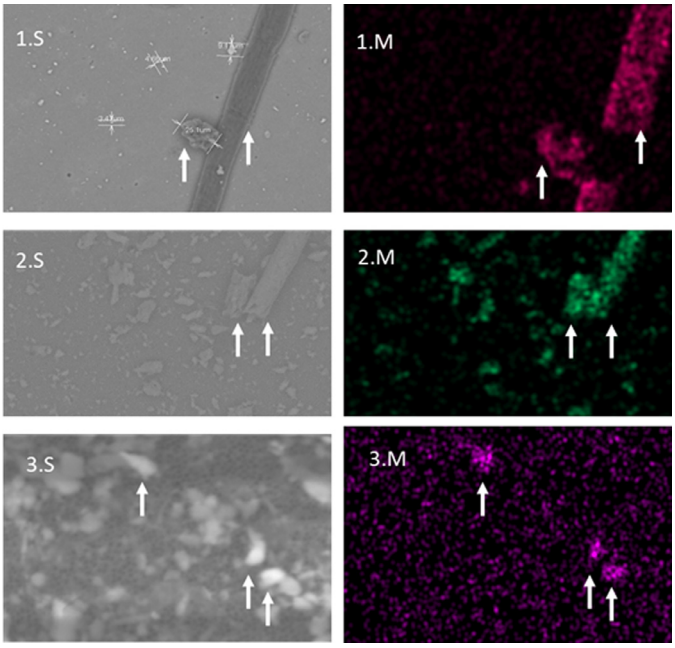

Fig. 4. Shows SEMs images 1.S, 2.S and 3.S (face masks 3, 7c and 4) and a corresponding elemental map (1.M, 2.M and 3 M). 1.M coloured fuchsia representing carbon on a fiber and particle, 2.M is coloured green to represent silica on grains and 3.M is Purple indicating the presence of lead found on some of the grains.

for heavy metal and organic compound leaching (suspected organic dyes). For comparative studies, a blank control using deionised water was run (same used in the leaching procedure), along with two plain standard face masks type I and II (mask 5, 6) to see if there was significance from novelty and plain face masks. In total, 8 DPFs were selected and placed in 250 mL deionised water and left submerged for 24 h. A procedural blank (deionised water taken through procedure) and reagent blank (deionised only) was also sampled to ascertain the quality of the background interference derived from the deioniser and glassware. A subsample of the leachate was analysed on ICP-MS and LC-MS using parameters mentioned in section 2.1.4.

For ICP-MS analysis of samples, a full external calibration was preformed to determine analyte concentration, and reagent and procedural blanks were used prior and post analysis of samples to assess potential carry over. All QC determinants for Cd, Co, Cu, Pb, Sb, and Ti passed acceptance criteria and blank samples possessing concentration values below the analytical detection limits (See supportive evidence). Table 3 shows the leachable heavy metals from the DPFs determined by ICP-MS analysis of the sub sampled water, with concerning levels of Sb released from festive novelty face masks (7a,b,c) and ranging from 111–393 µg/L. Additional to this, all face masks appeared to release Cu with levels ranging from 0.85 µg/L (Mask 5) to highest levels of 4.17 µg/L (face mask 2). Copper is a known environmental pollutant which can induce toxic effects in a number of organisms including humans (Keller et al., 2017; Rehman et al., 2019). Lastly, leachable Pb was present in samples 2–7a, interestingly the highest value of 6.79 µg/L was associated with face mask 6, the plain face mask purchased from Tesco © (see Table 3 for more details). Lead is a serious cause of concern and has known carcinogenic and toxicological effect on organisms and has potential to bio-accumulative, even low exposures to lead can have adverse side effects to humans, such as neurological damage and detrimental to foetal development (Freedman et al., 1990; Gundacker and Hengstschläger, 2012; Tchounwou et al., 2012). Looking at the wider picture, the vast amount of DPFs generated due to the COVID-19 pandemic could easily see the cumulative release of these elements breaching

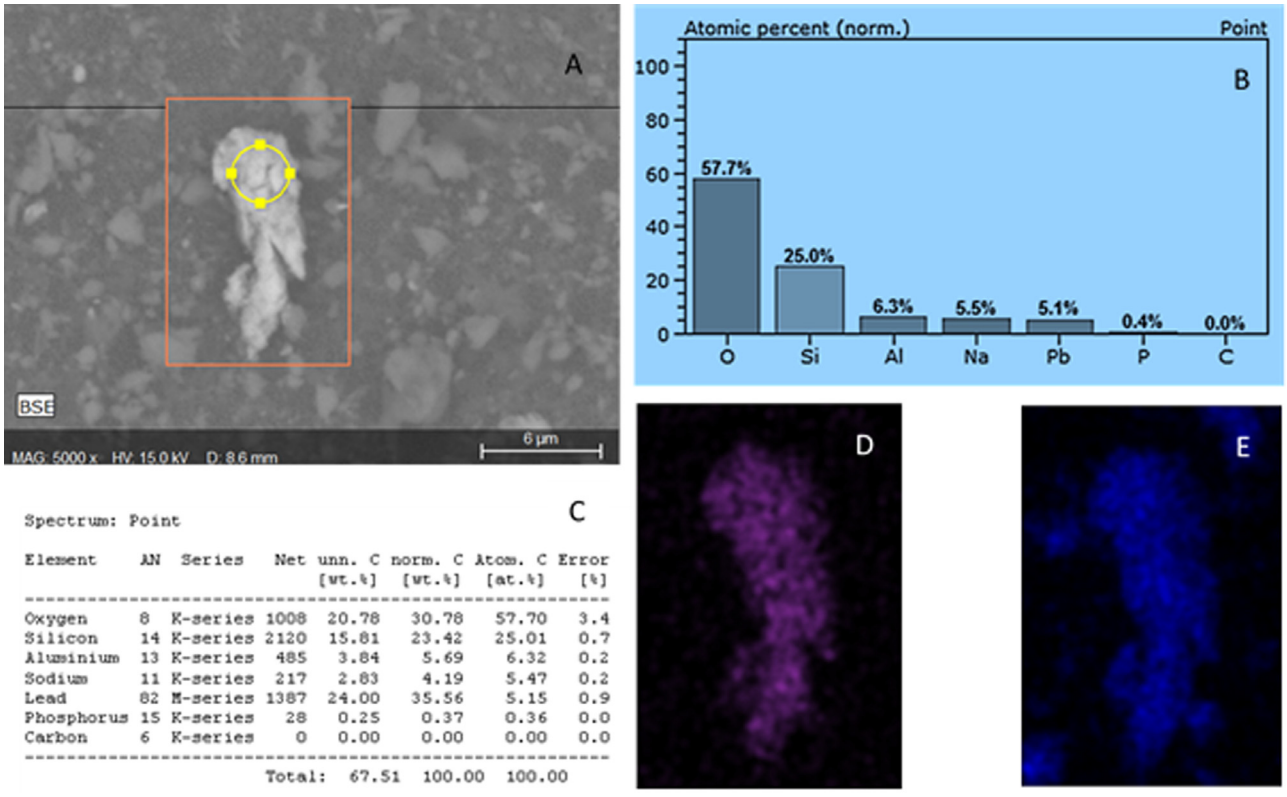

C

Spectrum: Point

Element	AN	Series	Net	unn. C [wt.%]	norm. C [wt.%]	Atom. C [at.%]	Error [%]
Oxygen	8	K-series	1008	20.78	30.78	57.70	3.4
Silicon	14	K-series	2120	15.81	23.42	25.01	0.7
Aluminium	13	K-series	485	3.84	5.69	6.32	0.2
Sodium	11	K-series	217	2.83	4.19	5.47	0.2
Lead	82	M-series	1387	24.00	35.56	5.15	0.9
Phosphorus	15	K-series	28	0.25	0.37	0.36	0.0
Carbon	6	K-series	0	0.00	0.00	0.00	0.0
		Total:		67.51	100.00	100.00	

Fig. 5. Is an example of EDX data referring to the composition of a grain particle found in face mask 4 (paw patrol). (A) is the image generated by the SEM at x5000, (B) shows the EDX data plotted graphically, whilst C is tabulated elemental composition data. Image D is false color map for elemental lead (Purple) and image E (blue) is an elemental map of Si the same grain.

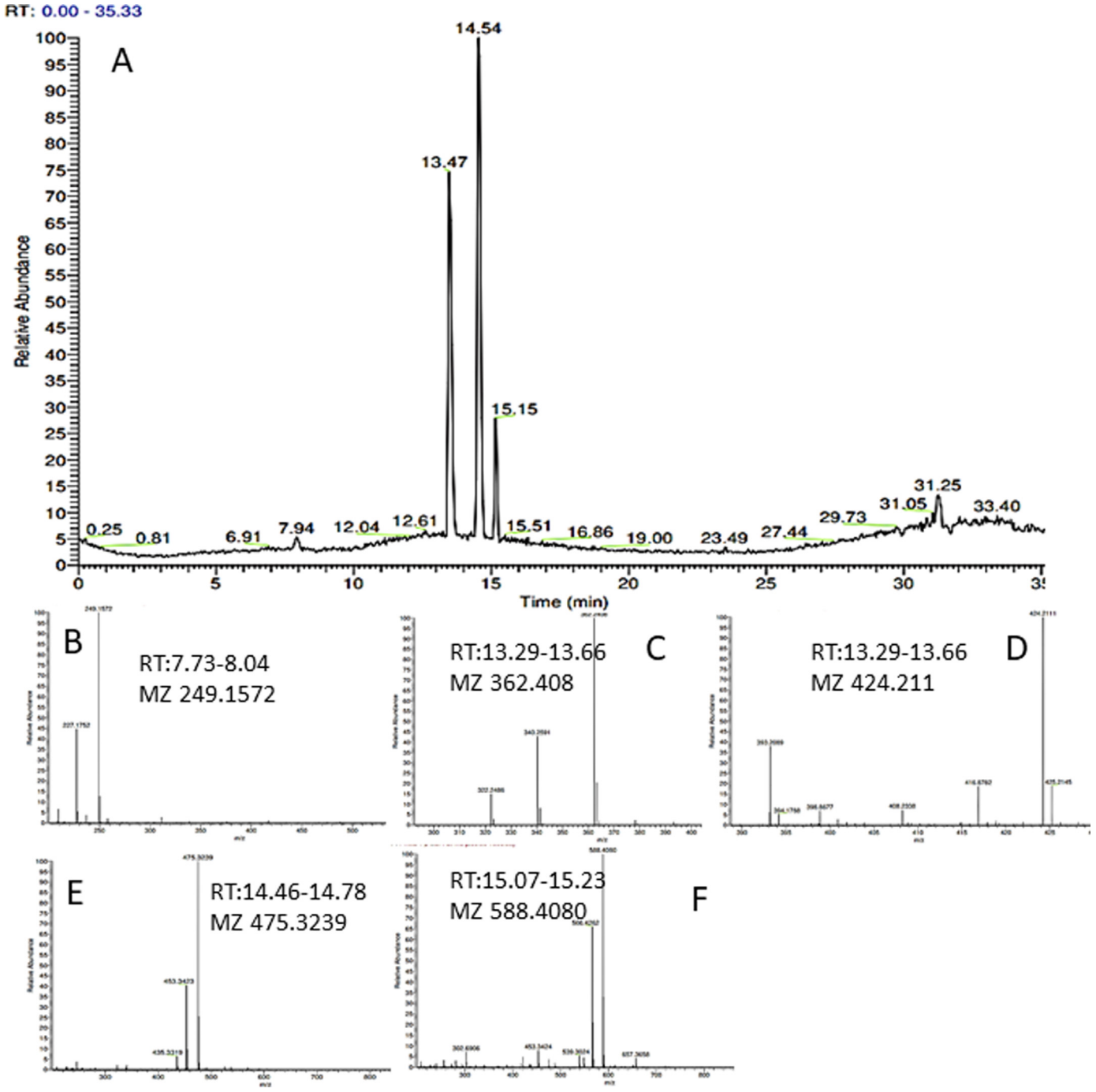

Fig. 6. Shows LC-MS data obtained from Leachate sample from face mask 4. Top A is the total ion chromatogram (TIC) and B-F are mass spectrums for the associated peaks of the TIC. Peak at Rt 7.73 has a mz of 249.1572 (B) was tentatively identified as Caprolactam. Mass spectrums C, D, E and F are therefore, likely to be oligomers of Caprolactam. More information regarding peak identity is found on table 4.

current guideline limits, in addition to this, there is a potential worry for the face mask wearers, who are potentially being exposed to heavy metals with no time dependant exposure data available.

In addition to heavy metal release, of the face masks analysed by LCMS (accurate mass), all emitted polar organic species of which, some tentatively identified as polyamide-66 ($[M + H]^+$ mz= 227.1754. $C_{12}H_{23}O_2N_2$), polyamide-6 and various oligomers of polyamide (PA), typically associated with nylon (Fig. 6). Nylon is often used in the elasticated parts of the DPFs and may be used interwoven in various layers of the face covering. PA-66 and PA-6 monomers and oligomers were identified ($[M + H]^+$ mz=340.2590 and 453.3421) (Tran and Doucette, 2006), in novelty face masks 4, 6, 7 a, b, c and in plain face mask 6 purchased from Tesco©. Medical type II mask (face mask 5) and black color face mask (6) showed little evidence of PA emission and is therefore likely to contain little, if any, nylon parts used in their fabrication. Of the compounds identified in the leachates, none of these species were identified in the procedural blank. The procedural blank was injected between samples to assess the potential background and carryover. The results of the blanks confirmed that there was no carryover between samples, and the background for each run was

Table 4
A table of LC-MS ions and there tentatively identified compound, preformed on the DPF leachates. Elemental formula takes into account of $[M + H]^+$ or $[M+Na]^+$ ion formation.

Accurate mass ions identified	Possible Elemental formula $[M+H]^+$ or $[M+Na]^+$	Tentatively identified contaminants	Present in samples
227.1754	$C_{12}H_{23}O_2N_2$	Caprolactam (PA66 monomer)	Face masks 4, 6, 7a,b,c
249.157	$C_{12}H_{22}O_2N_2Na$	P66 $[M+Na]^+$	
322.2485	$C_{18}H_{32}O_2N_3$	Unkown	
340.2590	$C_{18}H_{34}O_3N_3$	PA6 trimer	
362.2407	$C_{18}H_{33}O_3N_3Na$	PA6 trimer $[M+Na]^+$	
424.2111	$C_{17}H_{35}O_5N_4$	Unkown	
453.3421	$C_{24}H_{45}O_2N_4$	PA66 dimer or PA6 tetramer	
475.3237	$C_{24}H_{44}O_4N_4Na$	PA66 dimer or PA6 tetramer $[M+Na]^+$	
588.4082	$C_{30}H_{55}O_5N_5Na$	PA6 Pentamer	
285.1707	$C_{16}H_{21}ON_4$	Aromatic pyrrole like compound	Face mask 6 7a
311.149	$C_{17}H_{19}O_2N_4$	Azo like compound refer to LC-UV	
371.2184	$C_{19}H_{26}O_2N_6$	olomucine ll like compound	
393.2002	$C_{19}H_{26}O_2N_6Na$	olomucine ll like compound $[M+Na]^+$	
534-987	$C_{2n}H_{4n+2}O_{n+1}$	PEG like derivatives	Face mask 2, 5, 7a,b,c
701.493	$C_{36}H_{66}O_6N_6Na$	PA 66 adducts or PA6 Hexamer adducts $[M+Na]^+$	Face mask 6
311.115	$C_{2n}H_{4n+2}O_{n+1}$	PEG derivative	
355.1784	$C_{2n}H_{4n+2}O_{n+1}$	PEG derivative	
377.1692	$C_{2n}H_{4n+2}O_{n+1}$	PEG derivative	
326.3775	$C_{21}H_{46}N_2$	N-Undecyl-1-undecanamine	Face mask 5
455.3327	$C_{21}H_{47}N_2O_8$	N1-(2,5,8,11,14,17,20-Heptaoxadocosan-22-yl)-N1-(2-methoxyethyl)-N2-methylethane-1,2-diamine	
527.3892	$C_{25}H_{52}O_5N_6Na$	N-(7-Aminoheptyl)glycyl-N-[(2S)-6-amino-1-(carboxyoxy)-2-hexanyl]-N^2-(7-aminoheptyl)glycinamide* $[M+Na]^+$	

clear of the ions present in the samples. In some samples polyethylene glycol-like (PEG) derivatives were tentatively identified; in black color face mask (2) plain face masks (5, 6) and novelty face masks (7 a, b, c). PEG was not found in novelty children face mask 4 and in any of the procedural blank samples. PEG ($C_{2n}H_{4n+2}O_{n+1}$) is typically represented by a homologous series with a repeating mass difference of *mz* 22 and 44. PEG are typical contaminates associated with membrane filters and is often seen in LCMS as Multiple species on the chromatogram. However, due to limited PEG speciation in the leachate samples, and PEG was not present in all samples (Novelty face masks 4 and blank sample) it is therefore likely that PEG originated from DPFs.

Other molecules that were tentatively identified, but difficult to confirm was aromatic amines compounds (azo like), which were seen only at low level in a few samples (6, 7a). The peak corresponds to Rt 20.16 (supporting S3) also showed some absorption band on LC-UV (diode array in the HPLC stack of the LC-MS), further evidence that this is of a dye type compound. N-Undecyl-1-undecanamine was also a likely candidate found in face mask 5, which is a primary long chain surfactant type molecule, likely used in softening of PP during manufacture. MS/MS fragmentation data confirms N-Undecyl-1-undecanamine (*mz* = 326.3775) as a likely candidate, as it shows a loss of the decyl group a through probable homolytic cleavage, leaving a charged residing around a methyl-1-undecanamine fragment ion (*mz* = 186.2214). No other dye compounds were identified in other samples and it is likely that if any dye compounds were present in the leachate, then they were at significantly low levels and methodology would need further optimization in order to identify them, such as preconcentration and instrument parameter optimization. Further exploratory tests are required for more accurate identification, of components emitted from DPFs such as GCMS for volatiles analysis, LCMS/MS

and NMR for structural elucidation of unknowns, but it is striking from preliminary data that these face masks are emitting organic compounds that may have adverse environmental fate and possibly have bioaccumulation properties (Hahladakis et al., 2018).

4. Conclusion

There is a concerning amount of evidence that suggests that DPFs waste can potentially have a substantial environmental impact by releasing pollutants simply by exposing them to water. DPFs release small physical pollutants such as micro and nano size particles; mainly consistent with plastic fibres and silicate grains, which are well documented to have adverse effects on the environment and public health. In addition to the physical particles, harmful chemicals such as heavy metals (Pb, Cd and Sb), and organic pollutants are also readily released from. the DPFs when submerged in water. Many of these toxic pollutants have bioaccumulative properties when released into the environment and this research shows that DPFs could be one of the main sources of these environmental contaminants during and after the Covid-19 pandemic. It is, therefore, imperative that stricter regulations need to be enforced during manufacturing and disposal/recycling of DPFs to minimize the environmental impact of DPFs. Secondary to environmental concerns, there is a need to understand the impact of such particle leaching on public health, as all DPFs released micro/nano particles and heavy metals to the water during our investigation. One of the main concerns with these particles is that they were easily detached from face masks and leached into the water with no agitation, which suggests that these particles are mechanically unstable and readily available to be detached. Therefore, a full investigation is necessary to determine the quantities and potential impacts of these particles leaching into the environment, and the levels being inhaled by users during normal breathing. This is a significant concern, especially for health care professionals, key workers, and children who are mandated to wear masks for large proportions of the working or school day (6–12 h).

Declaration of Competing Interest

The authors declare that they have no known competing financial interests or personal relationships that could have appeared to influence the work reported in this paper.

Acknowledgements

This work has been supported by Dr Gareth Davies and Ms. Kate Johns of Tata Steel Europe group for ICP-MS analysis and Dr. Ann Hunter for LCMS analysis at National Mass Spectrometry Facility. We would like to acknowledge the grant supports from EPSRC (EP/R51312X/1; EP/N020863/1) and Swansea University Collage of Engineering. We would also like to thank to the Welsh Government Technical Advisory Group for their technical support and valuable feedback.

Supplementary materials

Supplementary material associated with this article can be found, in the online version, at doi:10.1016/j.watres.2021.117033.

References

Adyel, T.M., 2020. Accumulation of plastic waste during COVID-19. Science 369, 1314–1315. doi:10.1126/SCIENCE.ABD9925, (80-.).

Aragaw, T.A., 2020. Surgical face masks as a potential source for microplastic pollution in the COVID-19 scenario. Mar. Pollut. Bull. 159.

Bartošová, A., Blinová, L., Sirotiak, M., Michalíková, A., 2017. Usage of FTIR-ATR as non-destructive analysis of selected toxic dyes 25, 103–111.

Bhagat, J., Zang, L., Nishimura, N., Shimada, Y., 2020. Zebrafish: an emerging model to study microplastic and nanoplastic toxicity. Sci. Total Environ. 728, 138707. doi:10.1016/j.scitotenv.2020.138707.

Bianco, A., Passananti, M., 2020. Atmospheric micro and nanoplastics: an enormous microscopic problem. Sustain 12. doi:10.3390/SU12187327.

Bouwmeester, H., Hollman, P.C.H., Peters, R.J.B., 2015. Potential health impact of environmentally released micro- and nanoplastics in the human food production chain: experiences from nanotoxicology. Environ. Sci. Technol. 49, 8932–8947. doi:10.1021/acs.est.5b01090.

Charles, J., Ramkumaar, G.R., Azhagiri, S., Gunasekaran, S., 2009. FTIR and thermal studies on nylon-66 and 30% glass fibre reinforced nylon-66. E-J. Chem 6, 23–33. doi:10.1155/2009/909017.

Coates, J., 2006. Interpretation of infrared spectra, a practical approach. Encycl. Anal. Chem 1–23. doi:10.1002/9780470027318.a5606.

Fadare, O.O., Okoffo, E.D., 2020. Covid-19 face masks: a potential source of microplastic fibers in the environment. Sci. Total Environ. 737.

Freedman, R., Olson, L., Hoffer, B.J., 1990. Toxic effects of lead on neuronal development and function. Environ. Health Perspect. 89, 27–33. doi:10.1289/ehp.908927.

Fruijtier-Pölloth, C., 2012. The toxicological mode of action and the safety of synthetic amorphous silica-a nanostructured material. Toxicology 294, 61–79. doi:10.1016/j.tox.2012.02.001.

Gundacker, C., Hengstschläger, M., 2012. The role of the placenta in fetal exposure to heavy metals. Wiener Medizinische Wochenschrift 162, 201–206. doi:10.1007/s10354-012-0074-3.

Hahladakis, J.N., Velis, C.A., Weber, R., Iacovidou, E., Purnell, P., 2018. An overview of chemical additives present in plastics: migration, release, fate and environmental impact during their use, disposal and recycling. J. Hazard. Mater. 344, 179–199. doi:10.1016/j.jhazmat.2017.10.014.

Hineman, A., Purcell-joiner, R., 2010. Digestion , testing , and validation of heavy metals in cannabis. Perkin Elmer Appl. note 1–5.

Jung, M.R., Horgen, F.D., Orski, S.V., Rodriguez, C., V., Beers, K.L., Balazs, G.H., Jones, T.T., Work, T.M., Brignac, K.C., Royer, S.J., Hyrenbach, K.D., Jensen, B.A., Lynch, J.M., 2018. Validation of ATR FT-IR to identify polymers of plastic marine debris, including those ingested by marine organisms. Mar. Pollut. Bull. 127, 704–716. doi:10.1016/j.marpolbul.2017.12.061.

Jung, S., Lee, S., Dou, X., Kwon, E.E., 2021. Valorization of disposable COVID-19 mask through the thermo-chemical process. Chem. Eng. J., 126658.

Keller, A.A., Adeleye, A.S., Conway, J.R., Garner, K.L., Zhao, L., Cherr, G.N., Hong, J., Gardea-Torresdey, J.L., Godwin, H.A., Hanna, S., Ji, Z., Kaweeteerawat, C., Lin, S., Lenihan, H.S., Miller, R.J., Nel, A.E., Peralta-Videa, J.R., Walker, S.L., Taylor, A.A., Torres-Duarte, C., Zink, J.I., Zuverza-Mena, N., 2017. Comparative environmental fate and toxicity of copper nanomaterials. NanoImpact 7, 28–40. doi:10.1016/j.impact.2017.05.003.

Kögel, T., Bjorøy, Ø., Toto, B., Bienfait, A.M., Sanden, M., 2020. Micro- and nanoplastic toxicity on aquatic life: determining factors. Sci. Total Environ. 709, 136050. doi:10.1016/j.scitotenv.2019.136050.

Lellis, B., Fávaro-Polonio, C.Z., Pamphile, J.A., Polonio, J.C., 2019. Effects of textile dyes on health and the environment and bioremediation potential of living organisms. Biotechnol. Res. Innov. 3, 275–290. doi:10.1016/j.biori.2019.09.001.

Lin, W., Huang, Y.wern, Zhou, X.D., Ma, Y., 2006. In vitro toxicity of silica nanoparticles in human lung cancer cells. Toxicol. Appl. Pharmacol. 217, 252–259. doi:10.1016/j.taap.2006.10.004.

Lusher, A.L., Welden, N.A., Sobral, P., Cole, M., 2017. Sampling, isolating and identifying microplastics ingested by fish and invertebrates. Anal. Methods 9, 1346–1360. doi:10.1039/c6ay02415g.

Masuki, H., Isobe, K., Kawabata, H., Tsujino, T., Yamaguchi, S., Watanabe, T., Sato, A., Aizawa, H., Mourão, C.F., Kawase, T., 2020. Acute cytotoxic effects of silica microparticles used for coating of plastic blood-collection tubes on human periosteal cells. Odontology 108, 545–552. doi:10.1007/s10266-020-00486-z.

Murugadoss, S., Lison, D., Godderis, L., Van Den Brule, S., Mast, J., Brassinne, F., Sebaihi, N., Hoet, P.H., 2017. Toxicology of silica nanoparticles: an update. Arch. Toxicol. 91, 2967–3010. doi:10.1007/s00204-017-1993-y.

Paul, M.B., Stock, V., Cara-Carmona, J., Lisicki, E., Shopova, S., Fessard, V., Braeuning, A., Sieg, H., Böhmert, L., 2020. Micro- And nanoplastics-current state of knowledge with the focus on oral uptake and toxicity. Nanoscale Adv 2, 4350–4367. doi:10.1039/d0na00539h.

Prüst, M., Meijer, J., Westerink, R.H.S., 2020. The plastic brain: neurotoxicity of micro- and nanoplastics. Part. Fibre Toxicol. 17, 1–16. doi:10.1186/s12989-020-00358-y.

Rehman, M., Liu, L., Wang, Q., Saleem, M.H., Bashir, S., Ullah, S., Peng, D., 2019. Copper environmental toxicology, recent advances, and future outlook: a review. Environ. Sci. Pollut. Res. 26, 18003–18016. doi:10.1007/s11356-019-05073-6.

Song, Y.K., Hong, S.H., Jang, M., Han, G.M., Rani, M., Lee, J., Shim, W.J., 2015. A comparison of microscopic and spectroscopic identification methods for analysis of microplastics in environmental samples. Mar. Pollut. Bull. 93, 202–209. doi:10.1016/j.marpolbul.2015.01.015.

Sullivan, G.L., Gallardo, J.D., Jones, E.W., Hollliman, P.J., Watson, T.M., Sarp, S., 2020. Detection of trace sub-micron (nano) plastics in water samples using pyrolysis-gas chromatography time of flight mass spectrometry (PY-GCToF). Chemosphere 249, 126179. doi:10.1016/j.chemosphere.2020.126179.

Sungur, Ş., Gülmez, F., 2015. Determination of metal contents of various fibers used in textile industry by MP-AES. J. Spectrosc. doi:10.1155/2015/640271, 2015.

Tchounwou, P.B., Yedjou, C.G., Patlolla, A.K., Sutton, D.J., 2012. Molecular, Clinical and Environmental Toxicology, Molecular, Clinical and Environmental Toxicology, Experientia Supplementum. Springer Basel, Basel doi:10.1007/978-3-7643-8340-4.

Toussaint, B., Raffael, B., Angers-Loustau, A., Gilliland, D., Kestens, V., Petrillo, M., Rio-Echevarria, I.M., Van den Eede, G., 2019. Review of micro- and nanoplastic contamination in the food chain. Food Addit. Contam. - Part A Chem. Anal. Control. Expo. Risk Assess. 36, 639–673. doi:10.1080/19440049.2019.1583381.

Tran, J.C., Doucette, A.A., 2006. Cyclic Polyamide oligomers extracted from nylon 66 membrane filter disks as a source of contamination in liquid chromatography/mass spectrometry. J. Am. Soc. Mass Spectrom. 17, 652–656. doi:10.1016/j.jasms.2006.01.008.

Wilson, N., Corbett, S., Tovey, E., 2020. Airborne transmission of covid-19. BMJ 370, 10–11. doi:10.1136/bmj.m3206.

Wu, C.L., Zhang, M.Q., Rong, M.Z., Friedrich, K., 2005. Silica nanoparticles filled polypropylene: effects of particle surface treatment, matrix ductility and particle species on mechanical performance of the composites. Compos. Sci. Technol. 65, 635–645. doi:10.1016/j.compscitech.2004.09.004.

You, R., Ho, Y.S., Hung, C.H.L., Liu, Y., Huang, C.X., Chan, H.N., Ho, S.L., Lui, S.Y., Li, H.W., Chang, R.C.C., 2018. Silica nanoparticles induce neurodegeneration-like changes in behavior, neuropathology, and affect synapse through MAPK activation. Part. Fibre Toxicol. 15, 1–18. doi:10.1186/s12989-018-0263-3.